

ONLINE APPENDIX

Working from a Distance: Productivity Dispersion and Labor Reallocation

Jingping Gu Dongya Koh Andrew Liu
University of Arkansas

September 30, 2020

Contents

A	Alternative Measures of Work-From-Home	2
A.1	Share of Hours Working at Home.	2
A.2	Feasibility to Work from Home (Dingel and Neiman, 2020)	2
B	Real and Nominal Wage Responses to COVID-19	4
C	Non-parametric Estimation of Productivity	6
C.1	Methodology	6
C.2	Data and Empirical Results	7
D	Benchmark Model - Equilibrium Conditions	9
D.1	Wage Determination	9
D.2	Equilibrium Conditions in the Steady State	9
E	Quantitative Analysis	11

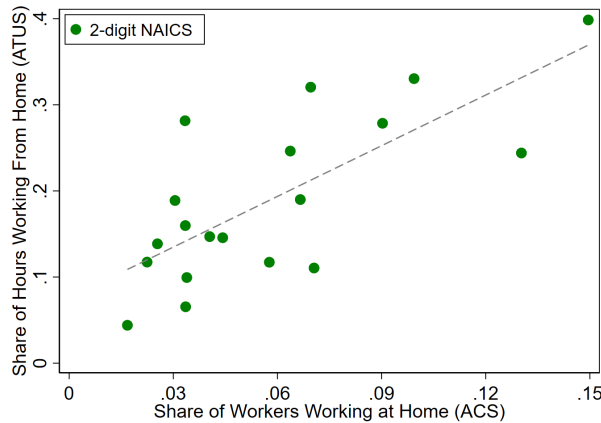
A Alternative Measures of Work-From-Home

A.1 Share of Hours Working at Home.

Another measure of adaptability to social distancing that resembles the one in our main text is a share of working hours from home by using the 2018 American Time Use Survey (ATUS) in BLS. ATUS data reports the amount of time people use for various activities. We utilize one of the survey questions that asks “Where were you while you were [ACTIVITY].” Using this information, we can calculate the share of the working hours of an average day people worked at home and aggregate this share by 51 industries or 2-3 digit industries.

In Figure A-1, we compare the ATUS measure of working from home with the ACS measure by the common 2-3 digit NAICS code. ACS measure is classified into 274 (sub-)industries, while ATUS measure is classified into 19 industries. Therefore, the comparison of the two measure is based on the 19 common industries in both data sets. The size of the ATUS measure is almost more than twice as the ACS measure. This is because ATUS measure is an intensive margin of working from home, while ACS measure is an extensive margin of working from home. The correlation of the two measures is 0.74.

Figure A-1: Comparing ACS Measure of WFH to ATUS Measure



Notes: Figure compares ACS measure of working from home with ATUS measure of working from home for the 19 common industries on both data sets. The dotted line indicates a linear line of the scatter plots.

A.2 Feasibility to Work from Home (Dingel and Neiman, 2020)

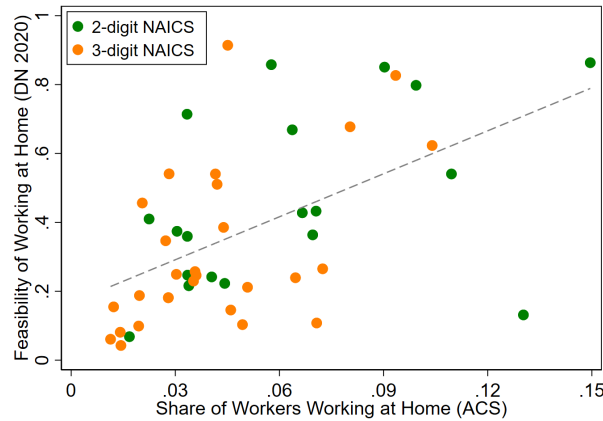
To justify the validity of the ACS measure as a proxy for the adaptability to social distancing, we can compare it with a measure developed by Dingel and Neiman (2020). They examine the economic impact of social distancing by constructing a measure that classifies the fea-

sibility of working at home for all occupations using two surveys administered by O*NET. Precisely, Work Context Questionnaire and Generalized Work Activities Questionnaire are used to capture interpersonal relationships, job characteristics, input of information, and work output. Each occupation is assessed whether or not the job can be done at home. They further aggregate this classification into 2-3 digit industry level (108 sub-industries).

Figure A-2 shows a comparison of the ACS measure to [Dingel and Neiman \(2020\)](#)'s feasibility measure by 2 and 3 digit industries. The comparison of the two measures is based on 47 common industries in both data sets. As is clear from the figure, there are some industries that DN measure assigns high feasibility value while we assign a low share value and vice versa. Two key industries in this comparison are again agriculture and education service sectors. The DN measure ranks the education services as the most feasible job that can be done at home, whereas they assign agriculture as the least feasible jobs to be done at home. Despite a few notable discrepancies between the two measure, it is clear that the ACS measure and the DN measure are positively correlated (0.53).

We confirm that the three measures above are all positively related and therefore can serve as a proxy for the adaptability to social distancing. Even though we keep using the ACS measure throughout the paper, our results remain unchanged with two other measures.

Figure A-2: Comparing ACS Measure of WFH to DN Measure



Notes: Figure compares ACS measure of working from home with DN measure of feasibility of working at home for the 47 common industries on both data sets. The dotted line indicates a linear line of the scatter plots.

B Real and Nominal Wage Responses to COVID-19

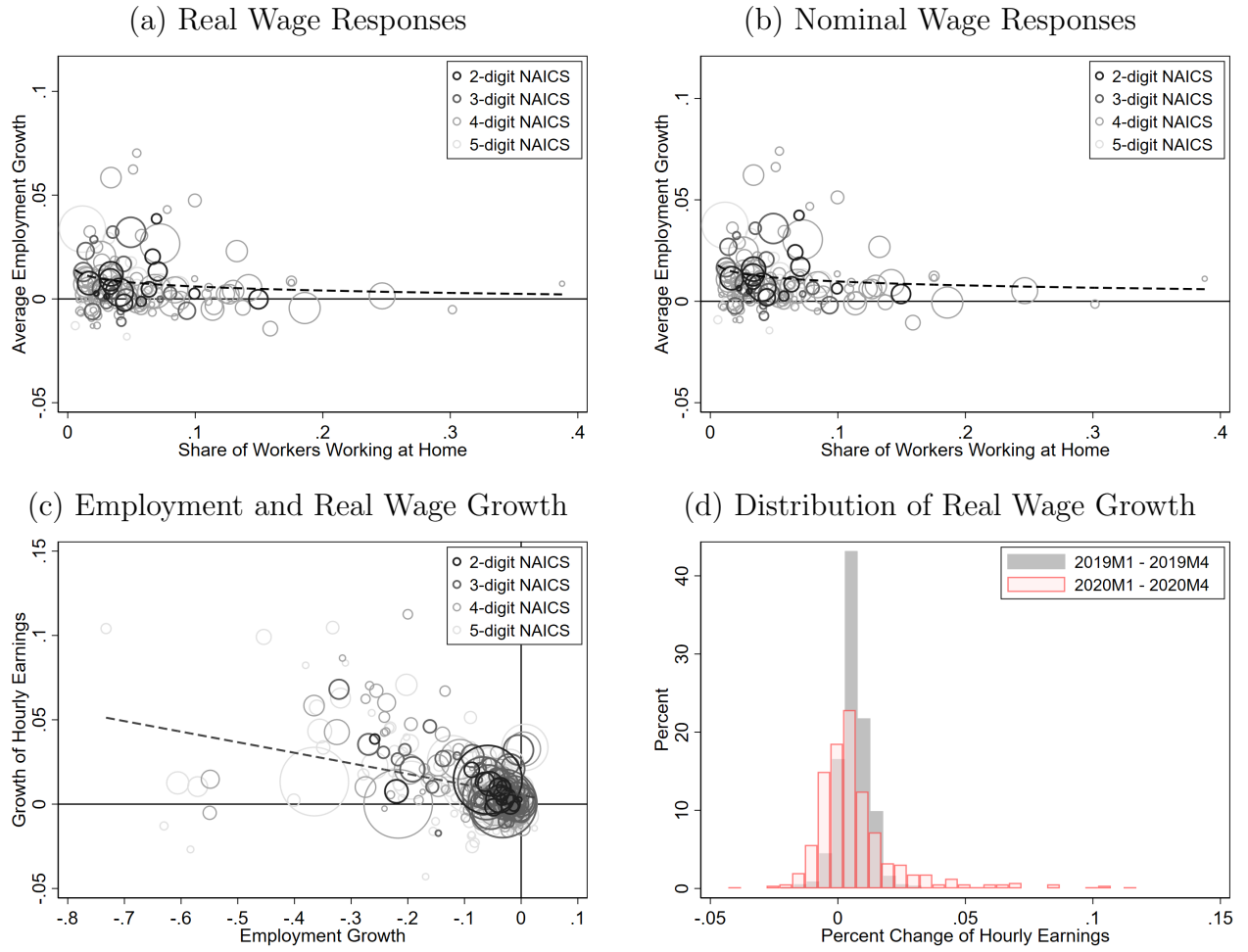
We document the responses of hourly earnings by industry right after the pandemic shock. We use BLS hourly earnings monthly data by industry to construct the wage growth before and after the outbreak of COVID-19. We construct real wage by denominating the nominal hourly earnings by the consumer price index for each month. Empirical evidence for the downward nominal wage rigidity by and in itself is of a growing interest in the literature. Panel (a) and (b) of Figure B-1 show the immediate response of real and nominal wage to the pandemic shock by the adaptability to social distancing. First, the nominal and real wage responses to the pandemic shock are very alike. Second, less adaptive industries have a more positive wage growth, both in real and nominal, than more adaptive industries. Third, the wage growth is more dispersed among less adaptive industries than more adaptive industries.

Panel (c) of Figure B-1 shows the relationship between wage growth and employment growth between January 2020 (2020M1) and April 2020 (2020M4) by industry.¹ We can observe a negative relationship between the two. Even though the wage responses are about 1/8 of employment growth, there is a statistically significant negative correlation. Interestingly, wage decline is almost little to none for most of the industries with a larger share of employment. The positive wage growth for the industries with a large employment decline is mainly due to laying off low-wage workers. The business closures and shutdowns induced by the pandemic shock enforces some firms and industries with limited adaptability to social distancing to lay off some workers. In this situation, low-wage workers or unskilled workers are likely to be laid-off first than skilled workers. As a consequence of the reduction in the number of low-wage workers, the average wage in the industry should slightly rise.

Panel (d) of Figure B-1 shows the distribution of wage growth from 2020M1 to 2020M4 comparing to the distribution a year ago, 2019M1 to 2019M4. Wage growth was all concentrated around zero or slightly positive a year ago. After the shock, however, the distribution slightly moves to the left but the mean is not significantly different from the distribution a year ago. What is different from a year ago is a dispersion of wage growth. After the pandemic shock, wage growth is more dispersed both on the positive and negative sides. Also, the concentration of almost-zero growth reduces to half.

¹BLS monthly data allows us to take the growth between January 2020 and April 2020, which captures the impact of COVID-19 shock more clearly than the growth between 2019Q4 and 2020Q1.

Figure B-1: Wage Responses and Dispersion



C Non-parametric Estimation of Productivity

C.1 Methodology

Another way of examining the dynamics of technical efficiency (TE) or productivity growth across industries is based on a nonparametric frontier analysis. We fit the data into envelopment models and technical efficiency measures as shown in [Färe et al. \(1994\)](#) and [Badunenko and Mozharovskyi \(2016\)](#) to estimate technical efficiency for each industry in each period.

We use the radial Debreu-Farrell output-based efficiency measurement ([Debreu \(1951\)](#) and [Farrell \(1957\)](#)) with an assumption of CRS technology. For each data point n , we use R different types of inputs x to produce S kinds of output y . Thus, (y, x) represents all feasible combinations of outputs and inputs. The maximum output or minimum input represents the Production Possibility Frontier under certain technology T .

For each observation n , we solve a linear programming problem:

$$\begin{aligned} \hat{G}_n(y_n, x_n; y, x | CRS) &= \max_{\theta, z} \theta \\ \text{s.t. } \sum_{n=1}^N z_n y_{ns} &\geq y_{ns} \theta_s, s = 1, 2, \dots, S; \\ \sum_{n=1}^N z_n x_{nr} &\leq x_{nr}, r = 1, 2, \dots, R; \\ z_n &\geq 0. \end{aligned} \tag{C-1}$$

where y is an $N \times S$ matrix for outputs data, and x is an $N \times R$ matrix of input data. In our analysis, for each specific industry, we have one output and two inputs—capital and labor.

There are some advantages of using a nonparametric analysis. First, the model allows more flexible functional form, and therefore, the Cobb-Douglass production function is no longer needed to estimate industry productivity. In this model, the technology efficiency is determined by the distance from each data to production possibility frontier. Second, the assumption on the perfectly competitive labor market is not needed. Since the model allows capital-labor ratio to change, the inefficiency we estimated in the model comes either from unbalanced capital and labor or from technological changes in the short run.

C.2 Data and Empirical Results

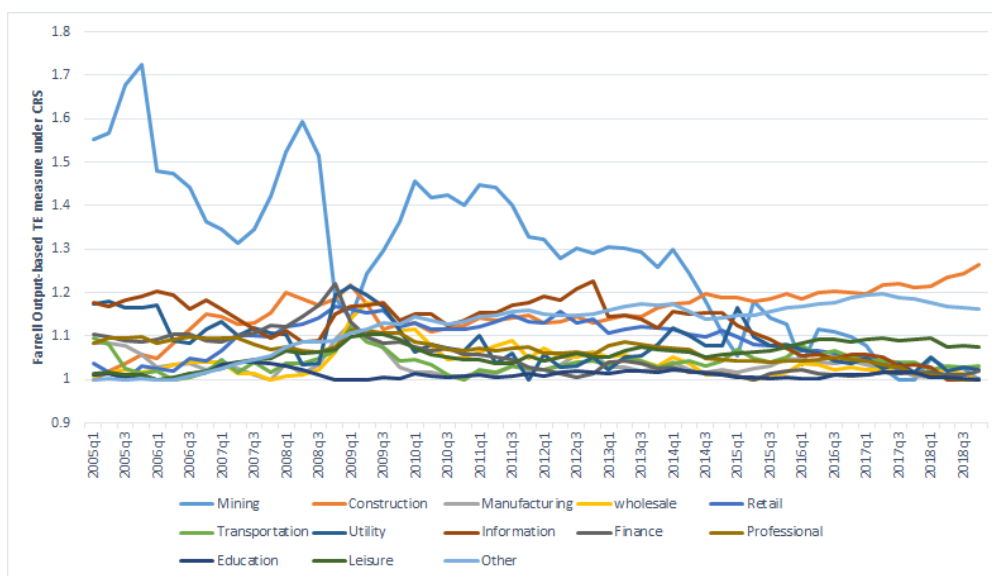
We use real value added in BEA GDP-by-Industry accounts for $Y_{i,t}$ as an output measure. For $K_{i,t}$, we use real net stock of capital for each industry from BEA Fixed Asset Table 3.2ESI. Since the fixed assets table in BEA is in annual data, we use Denton method (Fonzo and Marini (2012)) to interpolate the quarterly data. We use Employment by industry from BLS current employment statistics for $L_{i,t}$. All the data used in this nonparametric analysis is essentially the same as the data used in our accounting exercise in the main text.

We can observe the changes of technical efficiency over time for each industry in Figure C-1. The Technical Efficiency (TE) Measure shows the distance from production possibility frontier (PPF). Therefore, the larger number of TE measure indicates that the production is farther away from PPF, and hence, less efficient or lower productivity. “Mining and logging” industry shows an obvious downward trend of technical efficiency, which illustrates a clear improvement of technical efficiency from 2005 to 2018. The productivity of other industries remains relatively stable over the years despite some fluctuations around the mean. We observe a productivity decline in the majority of industries during the 2008 financial crisis.

We also estimate TE measure based on labor and value-added data of second quarter of 2020. For capital, we use 2018 capital data because the latest available industry data is 2018. We use 2019Q4 TE estimation comparing with TE in 2020Q2. A negative number means productivity decline from 2019Q4 to 2020Q2. We show the relationship between productivity and share of workers working at home in Figure C-2, which is consistent with Figure 1(b) in main text. We observe that a lower share of workers worked at home relates to a larger productivity decrease. The relationship is statistically significant. The point on bottom left corner of the figure is air transportation, which experienced dramatic productivity drop from 2019q4 to 2020q2.

We also try various ways to deal with capital data. For example, we use the same constant growth rate from 2017 to 2018 for each quarter to predict capital stock in each quarter of 2019 and first two quarters of 2020. Or, we forecast annual capital stock first and use the Denton method to stretch the annual data to the quarterly. For all these different ways to forecast capital, the consistent conclusion is obtained for the relationship between TE change and the share of workers worked at home.

Figure C-1: Technical Efficiency Measures: 2005-2018



Notes: The Technical Efficiency (TE) Measure shows the distance from production possibility frontier (PPF). Therefore, the larger number of TE measure indicates that the production is farther away from PPF, and hence, less efficient or lower productivity.

Figure C-2: Technology Efficiency Decline by the Adaptability to Social Distancing



Notes: Figure shows the TE changes from 2019Q4 to 2020Q2 by the adaptability to social distancing by 2-4 digit NAICS industry code. The size of each circle indicates the share of employment of each industry. The dashed line is a log-linear line.

D Benchmark Model - Equilibrium Conditions

D.1 Wage Determination

We follow [Chodorow-Reich and Wieland \(2020\)](#) and assume that the sector-specific wage is determined by Nash bargaining between the workers and the firms. Specifically, there is downward wage rigidity in the simple form that the nominal wage cannot fall by χ percent. Denote Π_i the gross producer price index, the market wage is determined by Nash bargaining scheme between firms and workers, w_i^* , but is constrained by the downward nominal wage rigidity:

$$w_i = \max\{w_i^*, (1 - \chi)w_{i,t-1}/\Pi_i\}. \quad (\text{D-1})$$

D.2 Equilibrium Conditions in the Steady State

In the steady state, the downward rigidity cannot bind because otherwise the price index has to decrease each period, which contradicts the steady state assumptions. The Nash bargaining wage then guarantees that the surplus of the workers and the firms are proportional in a way that $\frac{W-U}{\eta} = \frac{J}{1-\eta}$. Using this relation, we can solve for the steady state wage function:

$$(1 - \eta) [w_i - z + \beta(1 - \delta)(1 - f(\theta'_i))(W'_i - U'_i)] = \eta [p_i - w_i + \beta(1 - \delta)J'_i] \quad (\text{D-2})$$

and solve for w_i :

$$\begin{aligned} w_i &= (1 - \eta)z + \eta p_i - (1 - \eta)\beta(1 - \delta)(1 - f(\theta'_i))(W'_i - U'_i) + \eta\beta(1 - \delta)J'_i \\ &= (1 - \eta)z + \eta p_i - \eta\beta(1 - \delta)(1 - f(\theta'_i))J'_i + \eta\beta(1 - \delta)J'_i \\ &= z + \eta(p_i - z) + \eta\beta(1 - \delta)f(\theta')J'_i \\ &= z + \eta(p_i - z) + \eta\beta(1 - \delta)f(\theta')\frac{\kappa}{q(\theta'_i)}. \end{aligned} \quad (\text{D-3})$$

Fixing the market tightness, the reallocation shock decreases the workers' wage because it lowers the probability that the worker stays on the job, which decreases expected output. However, the reallocation shock necessarily changes the market tightness because the affected workers enter the unemployment pool, which increases the firms' expected value because of a decrease in queue length $q(\theta')$. The overall effect is ambiguous.

To obtain an equilibrium condition for steady state θ^* , we take $W_i - U_i$ which gives:

$$W_i - U_i = w_i - z + \beta(1 - \delta)(1 - f(\theta'_i))(W'_i - U'_i) \quad (\text{D-4})$$

and add J_i to the above equation:

$$\begin{aligned} V_i \equiv J_i + W_i - U_i &= p_i - z + \beta(1 - \delta)J'_i + \beta(1 - \delta)(1 - f(\theta'_i))(W'_i - U'_i) \\ &= p_i - z + \beta(1 - \delta)(1 - \eta)V'_i + \beta(1 - \delta)(1 - f(\theta'_i))\eta V'_i \\ &= p_i - z + \beta(1 - \delta)(1 - \eta f(\theta'_i))V'_i \end{aligned} \quad (\text{D-5})$$

where the second equation used Nash bargaining solution, $\frac{W-U}{\eta} = V = \frac{J}{1-\eta}$.

Finally, using the free entry condition, we have

$$\frac{\kappa}{(1 - \eta)q(\theta_i)} = p_i - z + \beta(1 - \delta)(1 - \eta f(\theta'_i)) \frac{\kappa}{(1 - \eta)q(\theta'_i)} \quad (\text{D-6})$$

In the steady state, this condition pins down θ_i^* :

$$\frac{\kappa}{(1 - \eta)q(\theta_i^*)} = \frac{p_i - z}{1 - \beta(1 - \delta)(1 - \eta f(\theta_i^*))} \equiv V_i^* \quad (\text{D-7})$$

Once we get the steady state θ_i^* , we can obtain steady state $(e_i^*, u_i^*, x_i^*, J_i^*, W_i^*, U_i^*)_{i \in N}$.

After pinning down the steady state market tightness, we can get the steady state value functions from the Bellman equations:

$$J_i^* = \frac{\kappa}{q(\theta_i^*)} \quad (\text{D-8})$$

$$U_i^* = \frac{z + \beta\theta_i^* \kappa \frac{\eta}{1-\eta}}{1 - \beta} \quad (\text{D-9})$$

$$W_i^* = \frac{\eta}{1 - \eta} \frac{\kappa}{q(\theta_i^*)} + U_i^* \quad (\text{D-10})$$

$$w_i^* = z + \eta(p_i - z) \frac{1 - \beta(1 - \delta)(1 - f(\theta_i^*))}{1 - \beta(1 - \delta)(1 - \eta f(\theta_i^*))} \quad (\text{D-11})$$

where the last steady state wage is coming from equation (D-4) solving for w_i and substitute in the equation (D-7).

E Quantitative Analysis

Calibration The calibrated parameters are shown in Table E-1. Most of the parameters are taken from [Chodorow-Reich and Wieland \(2020\)](#). Cost of vacancy (κ) and matching efficiency (M) are calibrated to match job finding rate $f(\theta) = 0.5$ and job filling rate $q(\theta) = 0.75$.

Table E-1: Calibrated Parameters

Separation rate	δ	0.066
Reallocation shock	λ	0.65
Industry reallocation noise	ρ	0.95
Discount factor	β	0.997
Bargaining power	η	0.6
Downward wage rigidity	χ	0.0035
Value of leisure	z	0.55
Cost of vacancy	κ	0.375
Matching efficiency	M	0.588

Impulse Responses of Labor Market Variables. We have discussed the counterfactual impulse responses of sectoral and aggregate unemployment with various persistence levels of productivity in sector 1 (α_1), reallocation frictions (λ), and the wage rigidity (χ) in the main text. In this section, we demonstrate all the impulse responses of labor market variables for each counterfactual exercise.

Figure E-1 shows the impulse responses of sectoral productivity, sectoral market tightness, sectoral job search, sectoral vacancy, sectoral unemployment, and aggregate unemployment to a one-time aggregate pandemic shock at $t=0$ for different persistence levels of productivity in sector 1. The solid lines indicate our benchmark case $\alpha_1 = 0.9$; the dashed lines for $\alpha_1 = 0.5$; and the dotted lines for $\alpha_1 = 0.1$. The dynamics of these variables with different persistence levels has been discussed in the main text.

Figure E-2 shows the counterfactual impulse responses of labor market to pandemic shock with different reallocation frictions. In our setting, the reallocation friction parameter λ lies in between 0 and 1 where $\lambda = 1$ indicates the perfect labor mobility across sectors, while $\lambda = 0$ indicates no labor mobility across sectors. Our benchmark reallocation friction was set at $\lambda = 0.65$.

Finally, Figure E-3 shows the counterfactual impulse responses of labor market variables

with different nominal wage rigidity. Our benchmark case assumes that nominal wage cannot decline more than $\chi = 0.0035$ percent of previous wage. In this exercise, we relax this rigidity to $\chi = 0.01$ percent (dotted lines) and $\chi = 0.1$ percent (dashed lines).

Figure E-1: The Persistence Level in Sector 1 (α_1)

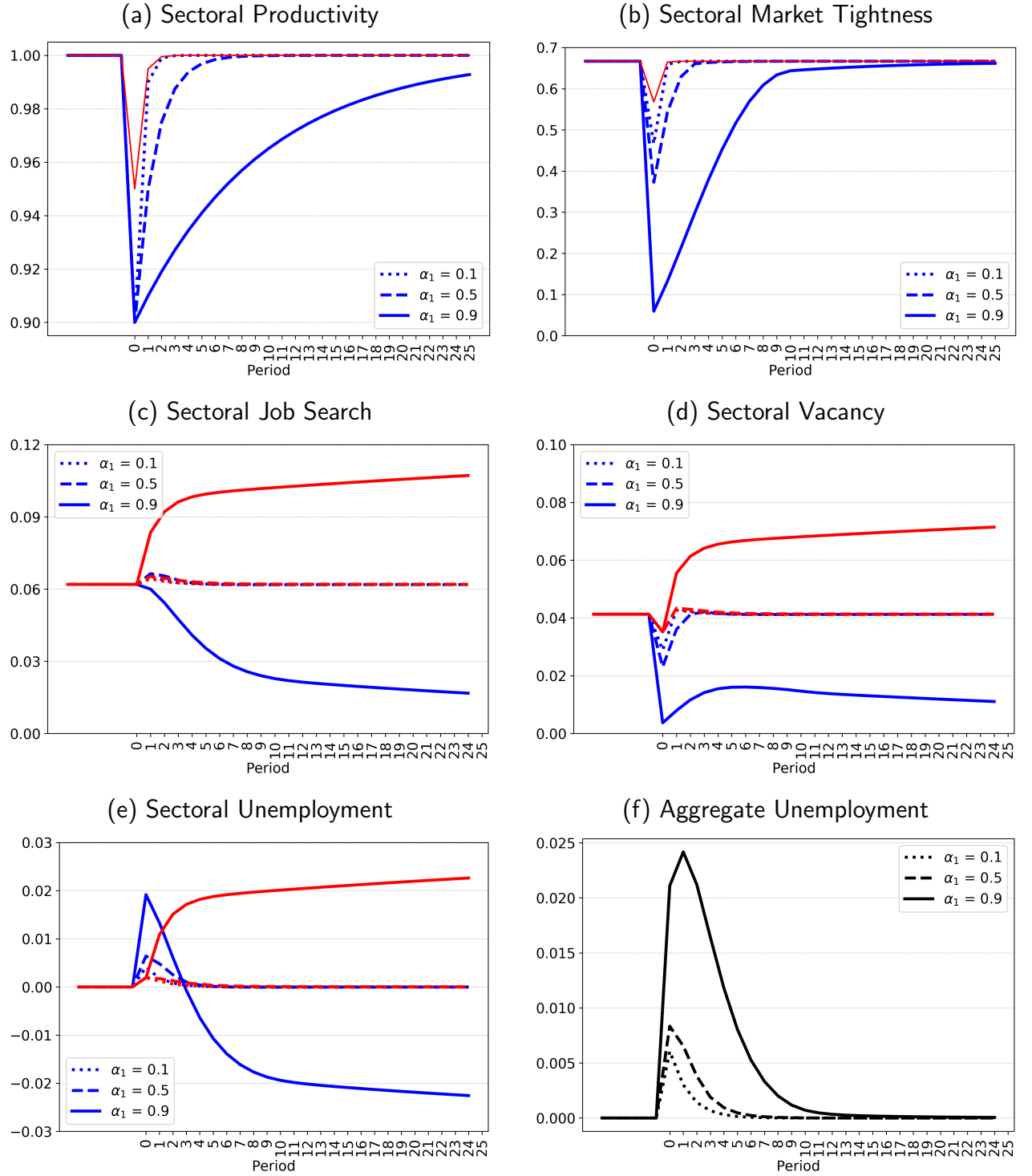


Figure E-2: Reallocation Friction across Sectors (λ)

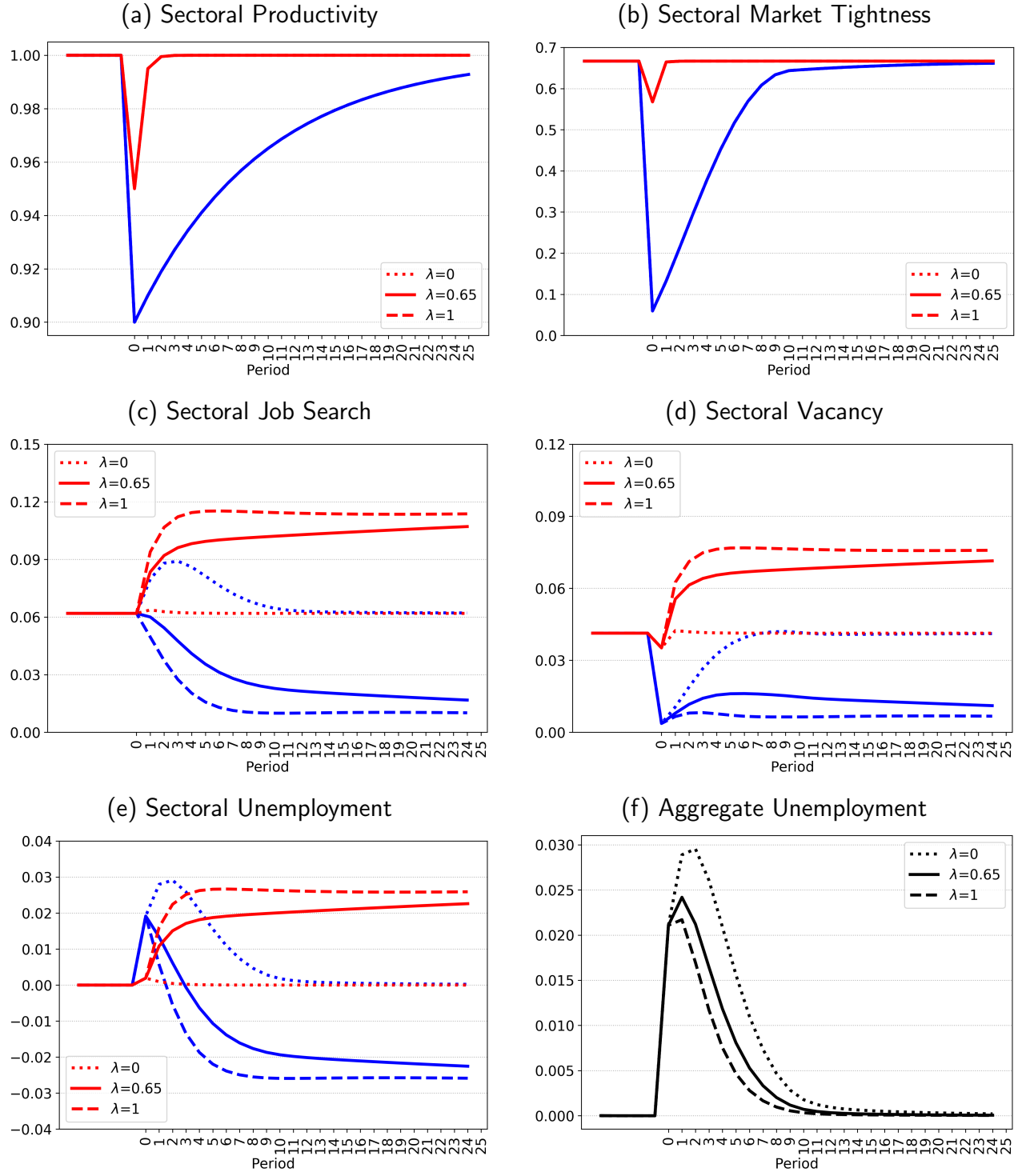
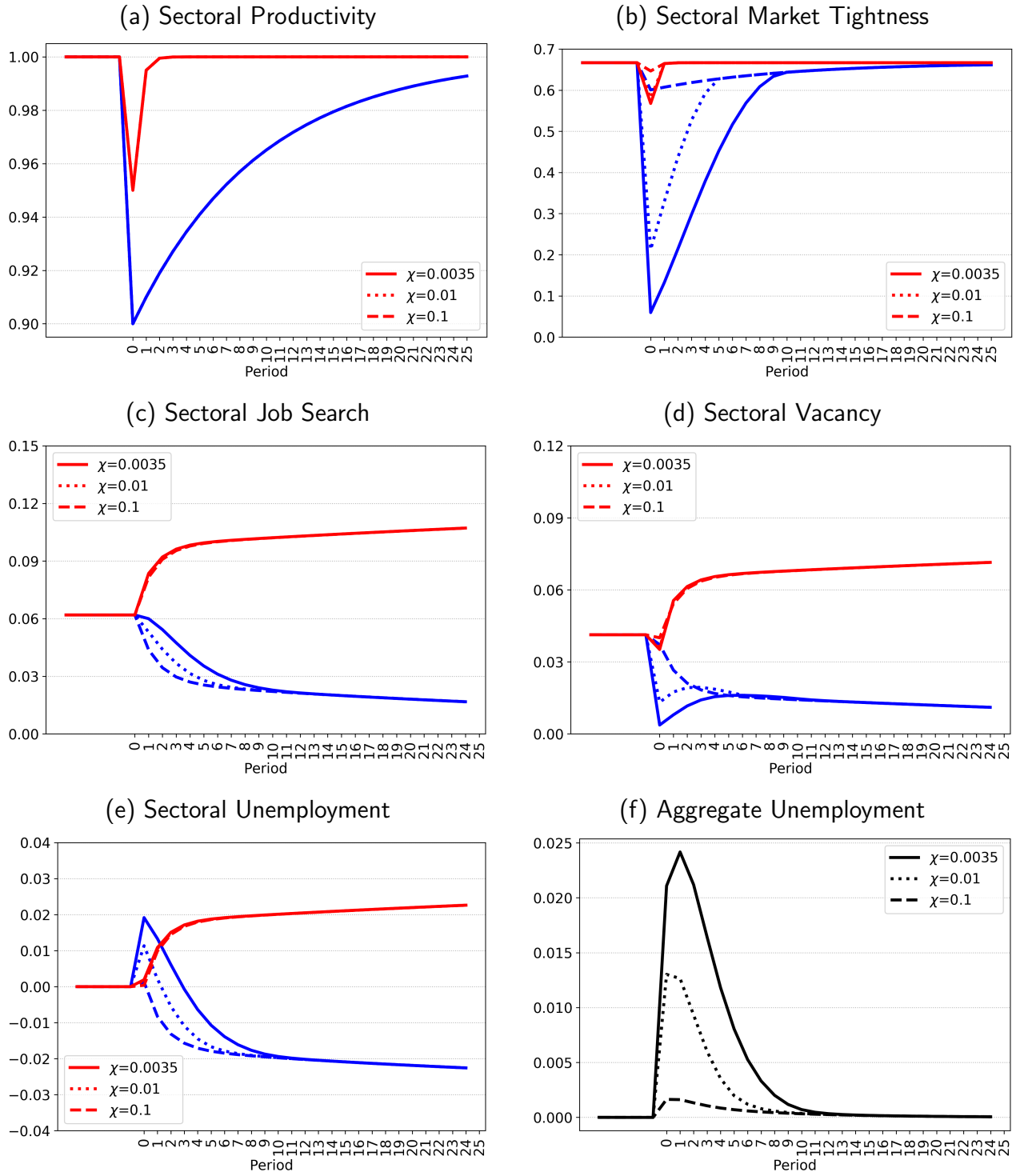


Figure E-3: Downward Nominal Wage Rigidity (χ)



References

- Badunenko, O. and Mozharovskyi, P. (2016). Nonparametric frontier analysis using stata. The Stata Journal, 16(3):550–589.
- Chodorow-Reich, G. and Wieland, J. (2020). Secular labor reallocation and business cycles. Journal of Political Economy, 128(6):2245–2287.
- Debreu, G. (1951). The coefficient of resource utilization. Econometrica, 19:273–292.
- Dingel, J. and Neiman, B. (2020). How Many Jobs Can be Done at Home? Journal of Public Economics, 189.
- Färe, R., Grosskopf, S., and Lovell, C. K. (1994). Production frontiers. Cambridge: Cambridge University Press.
- Farrell, M. J. (1957). The measurement of productive efficiency. Journal of the Royal Statistical Society, Series A 120:253–290.
- Fonzo, T. D. and Marini, M. (2012). On the extrapolation with the denton proportional benchmarking method. IMF Working Paper.